Determination of Magnet Specification of 13 MeV Proton Cyclotron Based on Opera 3D

Taufik[1*], A. Hermanto[2], P. Anggraita[1] and S. Santosa[1]
[1]*Center for Accelerator Science and Technology, National Nuclear Energy Agency*
Jl. Babarsari No.21, Po Box 6101 ykbb, Yogyakarta 55281, Indonesia
[2]*Department of Physic, Gadjah Mada University,*
Sekip Utara Bulaksumur, Yogyakarta 55281, Indonesia

ARTICLE INFO

Article history:
Received 03 March 2014
Received in revised form 22 May 2014
Accepted 30 May 2014

Keywords:
Supply some 4–6 keywords
Cyclotron magnet design
Positron emmision tomography
Proton 13 MeV
Opera 3D
Tosca

ABSTRACT

The magnet is one of the main components of a cyclotron, used to form a circular particle beam trajectories and to provide focusing of the beam. To support the mastery of 13-MeV proton cyclotron technologies, cyclotron magnet design must be done to satisfy cyclotron magnet requirements. This research was conducted by studying important parameters in designing the cyclotron magnet which is then used to determine the design requirements. The magnet design was based on the results of a 3D simulation using Opera 3D software. Opera 3D is a software developed by Cobham plc to solve physical problems in 3D such as magnetostatic using finite element methods. The simulation started by drawing a 3D model of the magnet using a modeler, followed by magnetic field calculations by Tosca module in the Opera 3D software. Simulation results were analyzed with the Genspeo software to determine whether the parameters of the cyclotron magnet have met design requirements. The results indicate that the magnet design satisfied the cyclotron magnet design requirement, that B in the median plane of the magnetic pole approached the isochronous curve, providing axial and radial focusing beam, crossing the resonance line at $\nu_r = 1$ when the particle energy is low and the particle energy is more than 13 MeV, and lead to small enough phase shift of about 13°. The dimension of the cyclotron magnet is 1.96 m × 1.30 m × 1.21 m; its weight is 17.3 ton; its coil current is 88,024 ampere-turn; its center magnetic field is 1.27479 T; its maximum magnetic field is 1.942116 T; its minimum magnetic field is 0.7689 T; its valley gap is 120 mm; its hill gaps are 40 to 50.78 mm; and its hill angles are 35° to 44°.

INTRODUCTION

One of the use of cyclotron in the health sector is as a provider of radioisotopes used in positron emission tomography (PET) imaging [1]. PET imaging produces a three-dimensional image of functional processes in the body.The PET system detects pairs of gamma rays emitted indirectly by a positron-emitting radionuclide (tracer) produced by cyclotron, which is introduced into the body on a biologically active molecule. Since the utilization of cyclotron in PET imaging in Indonesia is still low [2], cyclotron technologies need to be mastered, so that the provision and maintenance of cyclotron for PET can be done domestically with a higher local content. Additionally, mastering the cyclotron technologies is required for the development of the radiopharmaceutical and other cyclotron applications such as cyclotron for proton therapy. Therefore, in 2009, the Center for Accelerator and Material Process Technology (PTAPB)-BATAN began to study the development of cyclotron technology for PET systems. This activity is expected to generate cyclotron prototypes capable of producing radioisotopes for PET in 2019. This activity is divided into a number of activities based on the cyclotron components, one of which is the cyclotron magnet design. The magnet is a main component which serves to deflect the particle beam to a circular trajectory. Additionally, the cyclotron magnet focuses the beam, determining whether a sufficient portion of the proton beam hits the target.

Previously, we have performed preliminary calculations of a 13 MeV cyclotron magnet [3], but the work simply included analytical calculations using many assumptions, and did not include the determination of the detailed dimensions of the magnet. The conceptual design of the cyclotron was done to get the initial parameters of the cyclotron [4], but the results were still rough and needed to be detailed. It is difficult to analytically calculate the

* Corresponding author.
E-mail address:taufik@batan.go.id

distribution of the magnetic field at any point, but it can be done by numerical methods with the Opera 3D software and Tosca modules [5]. Therefore, the cyclotron magnet needs to be designed in detail so we can obtain a blueprint that can be used to construct a cyclotron magnet.

Based on the backgrounds, the problems to be solved in this research are how to determine the criteria of the cyclotron magnet and how to determine the dimensions of the magnet according to the criteria of the cyclotron magnet. In this study, the magnet design is based on three-dimensional magnetic field calculation, and the design results are not outlined in technical drawings. The purpose of this research is to obtain a design which can be used as a basis for the construction of the 13-MeV proton cyclotron magnet.

EXPERIMENTAL METHODS

Literature studies was conducted to determine the requirements for the cyclotron magnet design. The magnet design was approached using three-dimensional magnetic field simulations. The equipment used in this cyclotron magnet design was a computer equipped with Opera 3D software and Tosca module. The analysis of magnetic field can be done using the equilibrium orbit software such as Genspeo [6]. Magnetic field distribution data from Tosca simulation was used by Genspeo to get cyclotron magnet parameters. Genspeo was used to calculate magnetic field average and both axial and radial betatron oscillation. The steps of this research, organized into a flowchart, is shown in Fig. 1.

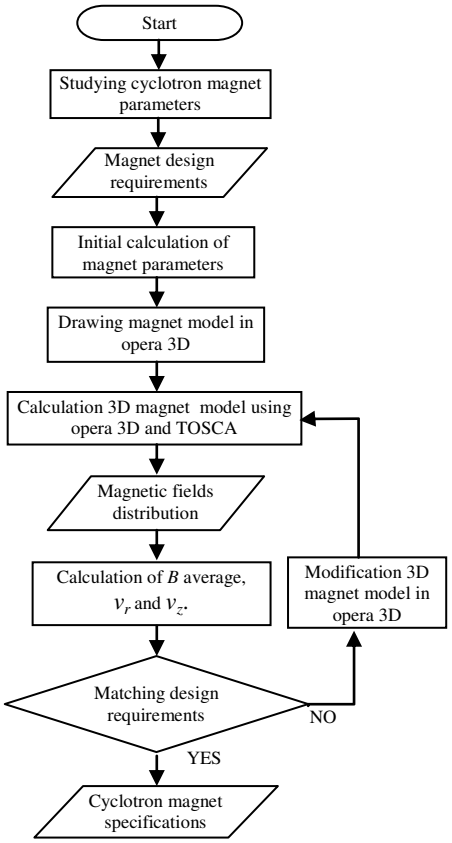

Fig. 1. Flowchart of research.

RESULTS AND DISCUSSION

Determination of design requirements

Cyclotron magnet design must meet the requirements formulated to guarantee that the proton energy can reach 13 MeV. High-energy protons can be produced by a cyclotron in two ways, namely by accelerating the protons themselves or by accelerating H^- ions. In H^- ions accelerating method, proton extraction can be done by passing H^- ions through a carbon foil (stripper) to convert it into an H^+ ion beam by stripping all of its electrons. The efficiency of extraction using carbon foils reaches 100% and do not cause electrical discharges [4]. In addition there are several advantages to use a carbon foil stripper, namely: (1) wider range of extracted proton energies, by changing the position of the carbon foil; (2) ability to be used in an ion source with a large current; (3) reduction of activation of components of the proton cyclotron; and (4) possibility of simultaneous extraction of protons with different energies [7]. Because the H^- ions acceleration method is more advantageous for the production of radioisotopes, it was determined that the type of accelerated particles is H^- ions and the extraction system uses a stripper. In the cyclotron, H^- ions generated by an ion source are placed in the central region of the magnetic poles. Based on considerations of ease of manufacturing, high efficiency ion beam, the cost of investment, and low maintenance costs [4], it was decided that the H^- ion source would be an internal ion source.

The other magnet design requirements are the magnetic flux density at the center of cyclotron (B_0) is determined to be 1.275 T and B average must satisfy isochronous conditions. Therefore, the magnetic materials must have a high hysteresis, low coercive force, and relatively low prices. Low-carbon steel satisfying the above criteria have been used in the Kirams-30 cyclotron; its hysteresis curve is shown in Fig. 2 [8]. To simplify the electromagnet manufacturing and the placement of the other cyclotron components, it was decided that the electromagnet system would be H shaped.

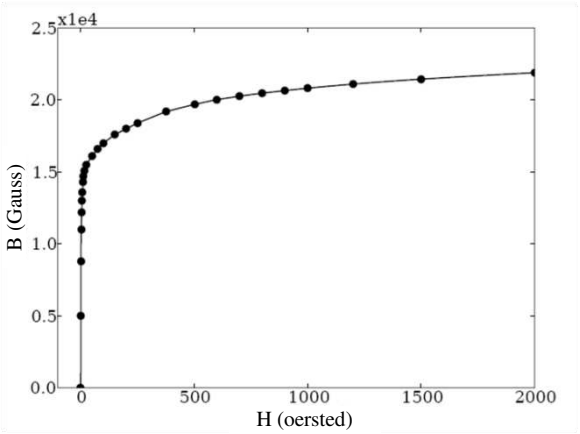

Fig. 2. Hysteresis curve of low-carbon steel [8].

The number of sectors (N) in this magnet design was decided to be 4, and the harmonic number (n_h) is 4. With the magnet having four sectors, magnet design is simplified and easier for placing two accelerator electrodes (dee) in the valley is made easier, so the hill gap can be smaller and a faster axial focusing is produced [9]. In this design, it was determined that the gap between the hills was to be 40 mm, and the valley gap was to be 120 mm. The axial and radial focusing are defined by radial betatron oscillation (ν_r) and axial betatron oscillation (ν_z), respectively. The operating point (ν_r, ν_z) moves as the particle kinetic energy increases and can cross the resonance lines. The resonances are dangerous when the crossing is slow (low kinetic energy gain per turn) [10]. As for N = 4 and energies below 15 MeV, the resonance lines which can damage the beams are ν_r=1, ν_r=2ν_z, ν_r=4/3 ν_z, ν_r=4/2 ν_z and 2ν_r+2ν_z=4 [9]. In the resonance region, the energy of motion in axial direction will be transferred to the radial, so that the size of the beam grows larger in the radial direction and vice versa.

Initial calculation of design parameters

Based on the design requirements, the accelerated particles in this cyclotron is H^- ion. When the H^- ions' kinetic energy (T) reaches 13 MeV, we have B_o = 1.275 T, and the particle orbit frequency (f) is 19.466 MHz. For n_h = 4, the RF frequency (f_{RF}) is 77.66 MHz. Inside the cyclotron, f_{RF} is always kept constant, therefore the magnetic flux density (B) must be isochronous. The isochronous B is calculated using the equation:

$$B(\rho) = \gamma B_0 = \frac{B_0}{\sqrt{1-\frac{\omega^2\rho^2}{c^2}}}, \qquad (1)$$

Where ρ is the radius of the trajectory, and for B_0 = 1.275 T, the isochronous B is shown in Fig. 3.

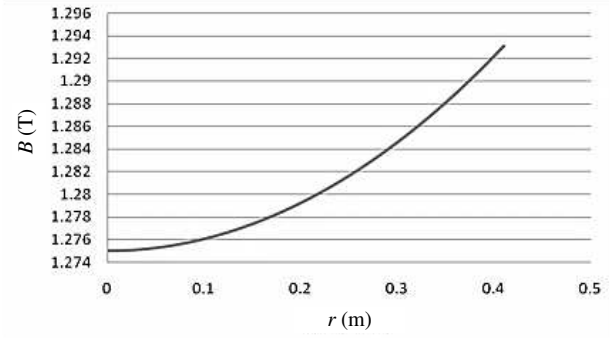

Fig. 3. Isochronous B for B_0=1.275 T.

To determine the radius of the magnetic poles (R), one needs to calculate magnetic rigidity ($B\rho$) which is defined in the equation

$$B\rho = \frac{E_o\gamma\beta}{cq}, \qquad (2)$$

with the speed of light c = 2.998 × 10^8 m/s. Based on equation (2), $B\rho$ at T = 13 MeV is 0.523062 T. Because B follows the relativistic factor γ, then B at T = 13 MeV is 1.292646 T. Thus, the radius of the trajectory (ρ) at T = 13 MeV is 0.404644 m. The radius of the magnetic poles is at least 0.404644 m, but due to edge effects, the polar radius must be greater than 0.404644 m.

Determination of magnet pole radius

B on the edge of the magnetic poles decreases in the radial direction. This is known as the edge effect. To estimate the edge effects in magnetic fields, calculations were performed with Opera-Tosca. The magnet was modeled with NI = 81 169 ampere-turn and flat magnetic poles with a gap 80 mm, while the pole radius (R) was varied. The graph of B against pole radius (r) is shown in Fig. 4.

Based on Figure 4, it appears that when the magnetic pole radius R = 0.404644 m, B decreased by 21.4% at r = 0.404644 m. In order for B at ρ = 0.404644 m is not affected by edge effects, then R must be enlarged. Therefore, the simulations were performed by varying R so that B at r = 0.404644 m would not decrease significantly. Based on the simulation results, at R = 0.48 m, B at r = 0.404644 m decreases by 0.48%.

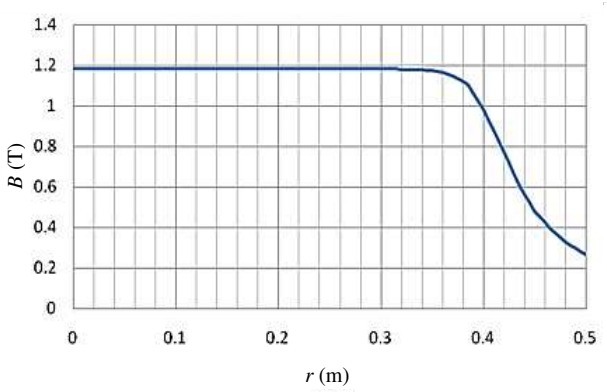

Fig. 4. *B* against r when pole radius R=0.4046 m.

Determination of return yoke width

A return yoke is a part of the magnet that serves to pass the magnetic flux. Larger cross-section areas of the return yoke lead to larger magnet dimensions and a greater weight of the magnet. Therefore, it is necessary to determine the effect of the cross-sectional width of the return yoke to *B* in the pole gap. In this design, the length of the return yoke is fixed at 1300 mm; consequently, varying the cross-sections area can be represented by varying the width of the return yoke. The calculation results are shown in Fig. 5.

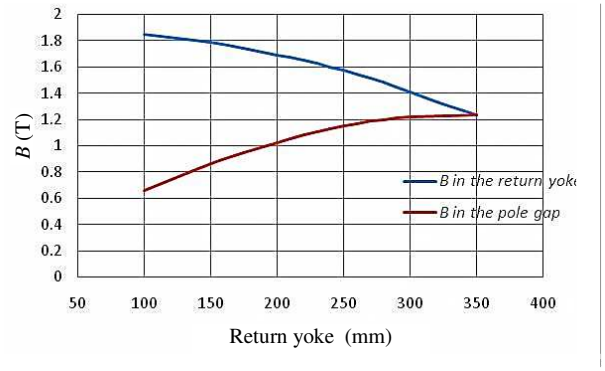

Fig. 5. *B* as function of the width of the return yoke curve.

Based on Figure 5, the width of the return yoke affects *B* in the pole gap. If the return yoke width is 100 mm, *B* in the return yoke reaches 1.85 T, which reaches the curved region of the hysteresis curve of Fig. 2. As a result, little magnetic flux passes through the return yoke, and *B* in the pole gap decreases greatly. For return yoke widths greater than 300 mm, it appears that *B* in the pole gap tends towards a saturation value. Based on consideration of its small dimensions and Fig. 5, the width of the return yoke was determined to be 250 mm. With this width, *B* in the return yoke in slightly above the linear region of the hysteresis curve, so the magnetic flux decline is small.

Determination of pole shape and the specification of cyclotron magnet

To fulfill the requirements of the 13 MeV cyclotron magnet design, the magnet model must be changed by varying the coil current, reducing the hill gap width at $r < 0.2$ m gradually and increasing the angle hill at $r > 0.2$ m gradually. After varying the magnetic poles shape and magnetic currents repeatedly, then magnetic models finally fulfilled the design requirements with the shape of magnetic poles shown in Fig.6.

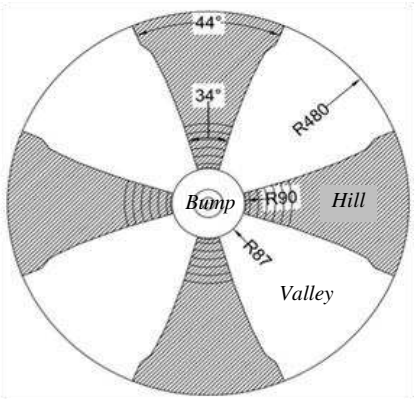

(a)

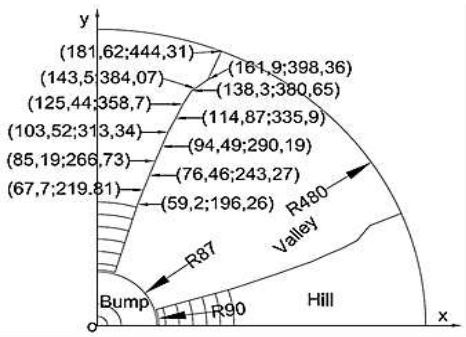

(b)

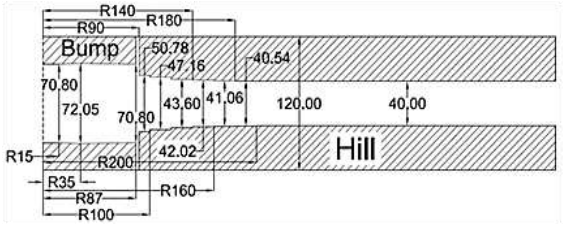

(c)

Fig. 6. The last model of cyclotron magnetic poles (a) Appear from median plane of the gap, (b) Hill side widening coordinate and (c) Side view of cyclotron magnet pole.

The magnetic model in Figure 6 was calculated for a coil current (*NI*) of 88,024 ampere-turn. The parameters from Genspeo calculation of the magnetic model were obtained by setting $B_0 = 1.27479$ T. The results are shown in Fig. 7.

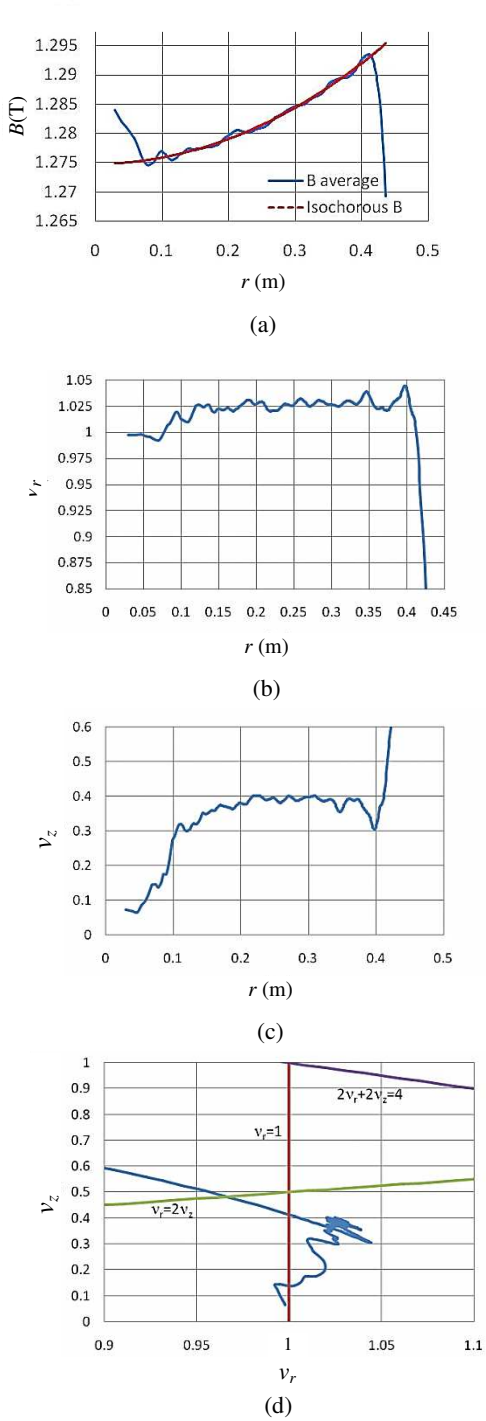

Fig. 7. The parameter of the final model of cyclotron magnet, (a) B average to r curve, (b) ν_r to r curve, (c) ν_r to r curve and (d) Tune diagram.

From the curve of B as function of r, it was found that B average is close to the isochronous curve with the largest margin of 10 gauss in the 0.06 m < r < 0.41 m region. Meanwhile, due to the bump, at r < 0.06 m, the difference between B average and isochronous curve reaches 88 gauss and decreases radially. This difference can be tolerated, because in the central region the turn separation is wide. Differences between B average with isochronous B in the central region is almost the same as in KIRAMS-13, namely 90 gauss [11].

Th ν_r vs r curve in Figure 7 has good characteristics. With values of 0.99 to 1.05, it provides a good radial focusing. Similarly for the ν_z vs r curve, as the ν_z values are positive, the beam always gets axial focusing along the trajectories. Futhermore, from the tune diagram, the curve crosses the resonance line twice at ν_r = 1. The intersection resonance line is still safe because the first intersection occurs when the particle energy is low and the turn separation is large, while the second intersection point occurs when the particles has been extracted. The tune diagram also intersects the resonance line at, but the intersection point occurs after the particles are extracted at 13 MeV so it will not damage the beam.

The phase shifts (ϕ) which occur in this cyclotron magnet design is shown in Fig. 8. The particle beams have a phase shift of about 13° at 0.05 m < r < 0.41 m. Referring to the KIRAMS-13 cyclotron, the phase shift achieved to about 15° [12], then the phase shift of our magnet design is already good. Meanwhile the phase shift in the central region is 45°. It is caused by the B average value in the bump which is larger than isochronous curve. The existence of a large phase shift in the central region can slow down the particles, so the radius of the trajectories are shifting. However, the turn separation in the central region is still wide so it will not damage the beams.

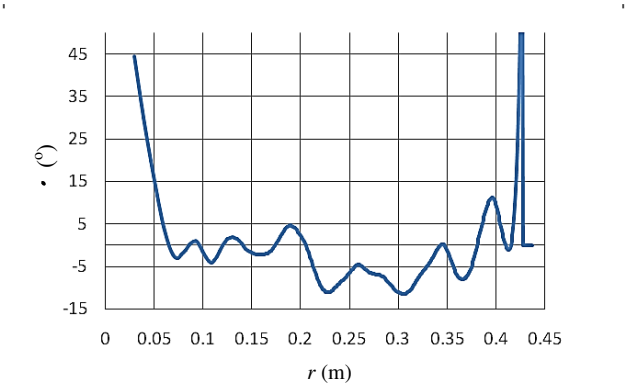

Fig. 8. Phase shift curve of the final model.

From the final simulation models, the dimension of the cyclotron electromagnet systems is 1.96 m × 1.30 m × 1.21 m as shown in Fig. 9, and the volume of the magnet material is 2,204,644,772 mm^3. By using the density of low carbon steel of about 7.85 g/cm^3 [13], the weight of the magnet materials was calculated as approximately 7.3 ton. The total current of the coil in the final simulation model is 2 × 44.012 ampere-turn. As B_o changes slightly from design

requirements, the RF frequency becomes 77.64 MHz. The design specifications of the 13 MeV proton cyclotron magnet are summarized in Table 1.

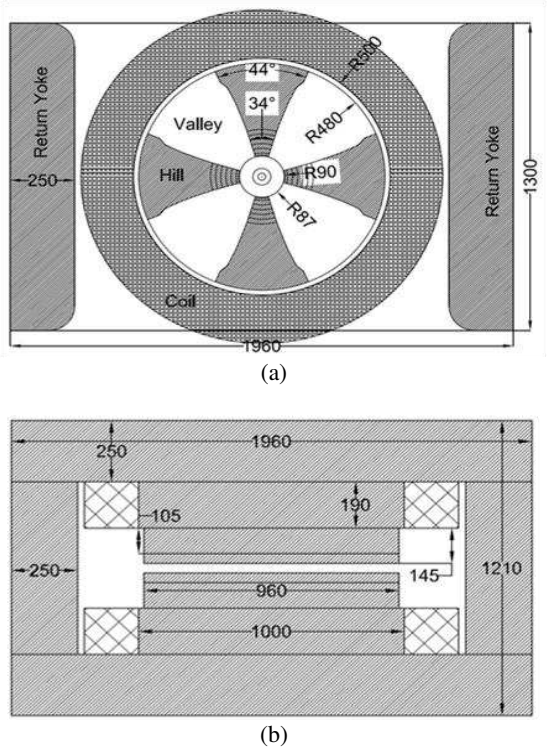

Fig. 9. Cyclotron magnet dimension (a) Median plane poles view and (b) Side view.

Table 1. The design specification of 13 MeV proton cyclotron magnet.

Proton kinetic energy	13 MeV
Accelerated ions	ion
Ion source type	internal
Sector number	4
Valley gaps	120 mm
Hill gaps	40 – 50.78 mm
RF frequency	77.64 MHz
B_0	1.27479 T
Maximum B_{hill}	1.942116 T
Minimum B_{valley}	0.7689 T
Coil current	2 × 44 012 ampere-turn
Poles radius (R)	0.48 m
Hill Angles	35° s.d. 44° from magnet center
ν_r(ν_r Average)	0.99 – 1.04391 (1.0256)
ν_z (ν_z Average)	0.07 – 0.40199 (0.36202)
Phase shift	± 13°
Magnet dimensions	1.96 m × 1.30 m × 1.21 m
Magnet weight (without coil)	17.3 ton

CONCLUSION

This research has created the 13 MeV proton cyclotron magnet design. The dimensions of the magnet are 1.96 m × 1.30 m × 1.21 m; its weight is 17.3 ton; its coil current is 88,024 ampere-turn; its center magnetic field is 1.27479 T, its maximum magnetic field is 1.942116 T; its minimum magnetic field is 0.7689 T; its valley gap is 120 mm; its hill gaps are 40 to 50.78 mm; and its hill angles are 35° to 44°. This magnet design satisfies the cyclotron magnet design requirement, that B in the median plane of the magnetic pole approaches the isochronous curve, providing axial and radial focusing beam, crossing the resonance line at $\nu_r = 1$ when the particle energy is low and the particle energy is more than 13 MeV, and leading to a sufficiently small phase shift of about 13°.

To complete this research, beam trajectory simulations were needed to determine whether the design of this magnet is able to produce 13 MeV protons. Further, as the magnet design used numerical approach, the shimming process of the constructed magnet will be based on the results of the measurements of the magnetic poles (mapping).

ACKNOWLEDGMENT

The authors would like to thank Joonsun Kang and Mohyun Yoon for discussions and suggestion about magnet design. The authors would also like to thank the State Ministry of Research and Technology for the financial support to meet those people.

REFERENCES

1. S.M. Qaim, Radiat. Phys. Chem. **71** (2004) 917.
2. H. Suryanto, *Particle Accelerator Technology Developments and Some of Their Applications*, Proceedings of Meeting and Scientific Presentations of Accelerator Technology and Its Application (2010) vii.
3. Saefurrochman, Taufik, A. Dwiatmaja, *et al*., *Initial Calculation of 13 MeV Cyclotron Magnet*, Proceedings of Meeting and Scientific Presentations of Accelerator Technology and Its Application (2009) 43. (in Indonesia)
4. Silakhudin and S. Santosa, Atom Indonesia **38** (2012) 7.
5. Cobham, Opera 3D User Guide, Vector Field Limited 24 Bankside Kidlington Oxford, England (2009) 9.

6. D.H. An, J.S. Chai, H.S. Chang, *et al*., *The Stripping Extraction System in The Kirams-13 Cyclotron*, Proceedings of APAC (2004) 111.

7. J.I.M. Botman and H.L. Hagedoorn, *Extraction from Cyclotron*, Proceeding of Cern Accelerator School (1996) 169.

8. J. Kang, B.H. Hong, D.H. An, *et al*., *Design Study of The 30 MeV Cyclotron Magnet*, Proceedings of EPAC (2006) 2559.

9. J.R. Richardson, Progress in Nuclear Techniques and Instrumentation, Volume 1, North-Holland Publishing Company, Amsterdam (1965) 3.

10. Y. Jongen and S. Zaremba, *Cyclotrons Magnet Calculations*, Proceeding Cern Accelerator School (1996) 139.

11. I.S. Jung, D.H. An, J.S. Chai, *et al*., *Design of Kirams-13 RF System for Regional Cyclotron Center*, Proceeding of Cyclotron and Their Applications (2004) 353.

12. S.H. Shin, M. Yoon, E.S. Kim, *et al*., J. Korean Phys. Society **45** (2004) 1045.

13. Anonymous, AISI 1015, http://www.efunda.com/materials/alloys/carbon_steels/show_carbon.cfm ID=AISI_1015&prop=All&Page_Title=Low-Carbon%20Steels, Retrieved in July (2013).